AD-A151 800 A COMPREHENSIVE STRATEGY FOR SATURATION DECOMPRESSION WITH NITROGEN-OXYGEN(U) DUKE UNIV MEDICAL CENTER DURHAM N C F G HALL LAB FOR ENVIRONM.. R D VANN 04 FEB 85 1/1

UNCLASSIFIED N00014-84-C-0163 F/G 6/19 NL

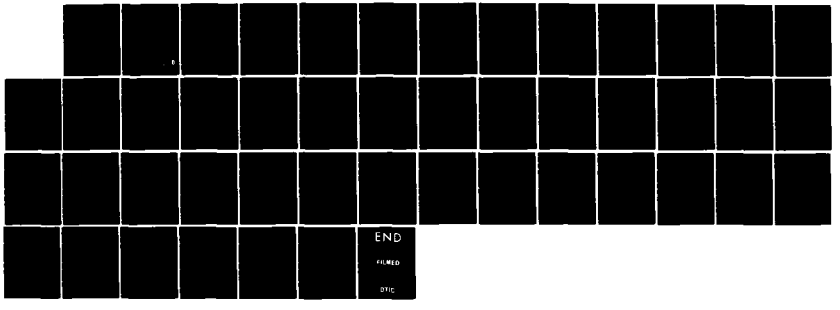

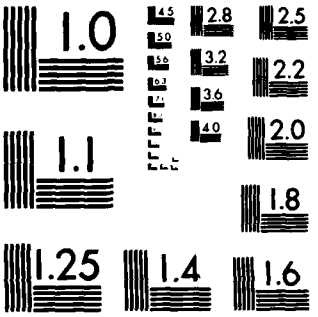

February 4,1985
Publication Manuscript

A COMPREHENSIVE STRATEGY FOR SATURATION DECOMPRESSION WITH NITROGEN-OXYGEN

Richard D. Vann, Ph.D.

F.G. Hall Environmental Research Laboratory
and
Department of Anesthesiology
Box 3823
Duke University Medical Center
Durham, North Carolina 27710

Contract N00014-84-C-0163

Workshop on Decompression from NITROX Saturation Diving

Conducted by the Undersea Medical Society, Inc.
Sponsored by the Office of Undersea Research, NOAA

January 8-9, 1985
Institute for Environmental Medicine
University of Pennsylvania

DEVELOPMENT OF SATURATION DECOMPRESSION SCHEDULES

Empirical Methods

Suppose we have divers saturated at some arbitrary depth, and we wish to decompress them to the surface (Fig. 1). Let us decompress at a constant rate of ascent. Upon surfacing, we find that the incidence of decompression sickness is 10%. On the next dive to the same depth, we choose a slower ascent rate for greater safety, and this results in a 5% incidence. If we use progressively slower ascent rates in future dives, we may presumably reduce the incidence of decompression sickness to any desired level. In this manner, saturation decompression schedules could be developed empirically with no recourse to theory. While not guaranteeing the most efficient schedules, the method would be easy to use with the ascent rate being the only undetermined parameter.

The Effect of Oxygen

How should the ascent rate be chosen? The literature indicates that several factors besides ascent rate affect the incidence of decompression sickness. One such factor is the inspired oxygen partial pressure which was studied by Vorosmarti, Hanson, and Barnard (1978) in a series of helium-oxygen saturation dives (Table 1). These dives used PIO2's of either 0.22 ATM or 0.4 ATM. With 0.22 ATM, there was a 52% incidence of decompression sickness. With 0.4 ATM, no decompression sickness occurred despite deeper dives and faster ascent rates.

Table 1. PIO2 and DCS risk.

PIO2 (ATM)	% DCS	Number of Dives	Mean Depth (FSW)	Mean Rate (FPH)
0.22	52	27	646	3.5
0.4	0	42	794	3.8

The influence of oxygen partial pressure on the risk of decompression sickness has been recognized for many years. Among numerous studies of the subject, two from the 1960's are useful here. One of these is Van Liew's demonstration that the rate of inert gas elimination from subcutaneous gas pockets in rats is proportional to the PIO2 (Van Liew et al. 1965; Van Liew et al. 1968). The other is the theoretical prediction by Workman (1969) and by Schreiner and Kelley (1967) that the ascent rate from a saturation dive is proportional to the PIO2 or

$$R = K * PIO2 \qquad (1)$$

where R is the ascent rate and K is the proportionality constant.

Let us adopt this latter hypothesis and call equation (1) the rate equation. By using progressively smaller values of K in succeeding dives, the incidence of decompression sickness could be reduced to any desired level as described earlier. The rate equation, therefore, should qualify as an empirical basis for developing saturation decompression schedules.

The rate equation can be integrated to find the form a decompression schedule assumes for either a constant oxygen partial pressure or a constant oxygen fraction (Fig. 2). When the PIO2 is constant, depth is a linear function of time

$$D(t) = Dsat - K * PIO2 * t/33 \qquad (2)$$

where Dsat is the saturation depth in FSW, t is time in hours, and K is measured in FPH/ATM. When the FIO2 is constant, however, the ascent rate decreases in proportion to the falling oxygen partial pressure, and depth is an exponential function of time

$$D(t) = (Dsat + 33\ FSW) * e^{(-K*FIO2*t/33)} - 33\ FSW \qquad (3)$$

The Effect of Saturation Depth

A second factor affecting the risk of decompression sickness is the saturation depth itself. This is shown in Table 2 where 152 air or nitrogen-oxygen decompressions are divided into groups having saturation depths of less than 100 FSW or greater than 100 FSW (Barry et al. 1984). The shallower group, with a mean depth of 62 FSW, had a 13% incidence of decompression sickness. The deeper group, with a mean depth of 151 FSW, had a 31% incidence even with slower ascent rates.

Table 2. Depth and DCS Risk

Mean Depth (FSW)	% DCS	Number of Dives	Mean Rate (FPH)
62	13	107	3.2
151	31	45	2.5

Why should the saturation depth affect the risk of decompression sickness? Let us suppose, as most evidence indicates, that decompression sickness is caused by undissolved gas and that the risk of decompression sickness rises with increasing gas volume. If we assume that gas evolves continuously during a linear ascent, we can conclude that the decompression risk increases with time as the gas volume expands.

This situation is illustrated in Fig. 3 where undissolved gas is represented by spherical bubbles. The bubble present after ascent from the deeper dive is larger than the bubble present after the shallower dive because more time is available for growth. Thus, for the same rate of ascent, the risk of decompression sickness is greater for the deeper dive.

If the ascent rate is reduced, gas evolves more slowly, and a smaller bubble develops. Schedule 1 in Fig. 4 has a slower ascent rate and a lower gas volume than schedule 2. Schedule 1 will have a lesser decompression risk than schedule 2.

Schedule 3 in Fig. 4 represents the effect of increasing the PIO2. A higher PIO2 permits a faster ascent rate with no additional bubble growth since, as Van Liew et al. (1965; 1968) demonstrated, increasing the PIO2 increases the rate of inert gas elimination.

What effect does saturation depth have upon the rate equation? Its form remains unchanged, but the magnitude of K decreases with increasing depth. This ensures that deeper dives will have the slower ascent rates they require to avoid unduely large bubbles.

A Quantitative Model of Bubble Growth and Resolution

The effects on ascent rate of saturation depth and oxygen partial pressure can be put into quantitative form with the aid of a simple model. The resulting theory can then be fit to experimental data using the likelihood method that was recently introduced to diving by Weathersby, Homer, and Flynn (1984).

Let us suppose, as shown in Fig. 5, that the volume V of a bubble increases in proportion to the ascent rate and decreases in proportion to the PIO2. The rate of change of the bubble volume is thus equal to the difference between the rates of increase and decrease

$$dV/dt = C1*R - C2*PIO2 \quad (4)$$

where C1 and C2 are proportionality constants. This relationship is readily integrated to find bubble volume as a function of time for constant PIO2

$$V = V0 + (C1*R - C2*PIO2)*t \quad (5)$$

where V0 is the initial bubble volume, and for constant FIO2

$$V = V0 + (C1*R - C2*FIO2*P0)*t + 0.5*C2*FIO2*R*t^2 \quad (6)$$

where P0 is the initial barometric pressure. Equations 5 and 6 apply when R is zero during decompression stops.

With these functions, it is possible to predict how the bubble volume will change during any decompression. Figure 6 shows the SCORE decompression schedule which resulted in 7 decompression incidents in 48 trials. The rate of bubble growth is rapid when the ascent rate is high. As the ascent rate is decreased, the bubble growth rate also decreases.

Likelihood and DCS Risk

In their discussion of likelihood, Weathersby et al. (1984) pointed out that as in pharmacology where the response to a drug can be related to the dose that is given, so the risk of decompression sickness can be related to the environmental parameters. This is illustrated in Fig. 7 by a dose-response curve which associates decom-

pression risk with bubble volume. Since bubble volume is a function of depth, gas mix, and ascent rate, the dose-response curve can predict the fractional risk for any decompression schedule.

The actual outcome of a decompression, however, does not have a fractional risk but rather a risk of either zero or one.

Theory	Experiment
$0 \leq P(DCS) \leq 1$	X = 1 if DCS
P(no-DCS) = 1 - P(DCS)	X = 0 if no DCS

Theory predicts that the probability of decompression sickness, P(DCS), will be between zero and one and that the probability of no decompression sickness will be 1 minus P(DCS). The experimental outcome which shall be defined as X, on the other hand, is 1 if decompression sickness occurs and 0 if decompression sickness does not occur.

This dichotomy is resolved by likelihood. Likelihood is the probability of an outcome. Thus, when decompression sickness occurs with an outcome X of 1, the likelihood is equal to P(DCS), the probability of decompression sickness.

If X = 1, likelihood = P(DCS).

When decompression sickness does not occur and the outcome X is zero, the likelihood is equal to P(no-DCS), the probability that decompression sickness does not occur.

If X = 0, likelihood = P(no-DCS).

Expressed quantitatively,

$$\text{Likelihood} = P(DCS)^{X} * P(\text{no-DCS})^{1-X} \qquad (7)$$

This formulation combines information from both theory and experiment. Indeed, likelihood is a measure of the error (or agreement) between theory and experiment as the following examples illustrate.

Consider a theory which is always correct. When decompression sickness occurs, this theory predicts that P(DCS) is one. Calculation shows that the likelihood also is one.

$$X = 1 \qquad P(DCS) = 1$$

$$P(DCS)^{X} * P(\text{no-DCS})^{1-X} = 1^{1} * 0^{0} = 1$$

When decompression sickness does not occur, the correct theory predicts that P(no-DCS) is one. Again, the likelihood is found to be one.

$$X = 0 \qquad P(DCS) = 0$$

$$P(DCS)^{X} * P(\text{no-DCS})^{1-X} = 0^{0} * 1^{1} = 1$$

Now consider a theory which is always incorrect. When decompression sickness occurs, this theory predicts that P(DCS) is zero. When decompression sickness does not occur, the incorrect theory predicts that P(no-DCS) is one. In both cases, the likelihood is zero.

$$X = 1 \qquad P(DCS) = 0$$

$$P(DCS)^{X} * P(\text{no-DCS})^{1-X} = 0^{1} * 1^{0} = 0$$

$$X = 0 \qquad P(DCS) = 1$$

$$P(DCS)^{X} * P(\text{no-DCS})^{1-X} = 1^{0} * 0^{1} = 0$$

The magnitude of the likelihood, between zero and one, is a measure of the error or agreement between theory and experiment. Likelihood allows the quantitative comparison of theories. These theories may be empirical or physiological.

Analysis of Experimental Data

The concept of likelihood may be extended to a series of observations by multiplying the likelihoods of individual observations. (This is analogous to finding the probability of a series of coin tosses by multiplying the probabilities of the individual tosses.) As the individual observations need not be made on the same decompression schedule, observations on all well-documented schedules may be used. The results of 21 air or nitrogen-oxygen saturation decompression schedules were found in the literature and are summarized in Table 3. These include a total of 233 man-decompressions in which there were 39 cases of decompression sickness for a mean incidence of 16.7%. Appendix A lists complete information on all schedules.

Table 3. Air and N2-O2 saturation decompression schedules.

Depth	DCS	Dives	Name	Reference
50	2	2	Pre-SHAD	Hamilton et al. (1982)
	0	2	SHAD I	
	1	3	SHAD III	
60	1	2	SHAD II	
	7	48	SCORE	Miller (1976); Philp et al. (1979)
	4	10	Dive 1	Thalmann (1984)
	3	10	Dive 2	
	1	10	Dive 3	
	1	10	Dive 4	
	1	11	Dive 5	
	1	20	Dives 6 & 7	
	0	10	Dive 8	
	2	23	AIRSAT 1 & 2	Eckenhoff and Vann (1985)
65	1	18	SUREX 65	
75	0	6	SUREX 75	
90	0	3	NOAA OPS I	Miller et al. (1976)
132	3	12	AIRSAT 3	Eckenhoff and Vann (1985)
	1	15	AIRSAT 4	
165	5	10	OI/NOAA	Barry et al. (1984)
197	5	6	NISAHEX	Muren et al. (1984)
198	0	3	NISAT I	Hamilton et al. (1982)

The bubble volumes occurring at the surface, or at the depth of decompression sickness, were found for each of these schedules as shown earlier for the SCORE decompression. From these volumes, the probabilities of decompression sickness were predicted using the Risk Function as a dose-response curve

$$P(DCS) = 1 - e^{(-C3 * V^{C4})} \qquad (8)$$

where V is the bubble volume and C3 and C4 are undetermined parameters. Having found the probabilities and knowing the experimental outcomes, the likelihood could be calculated for the whole series of schedules.

The magnitude of the likelihood is controlled by the values of the parameters C1 and C2 in the bubble model and C3 and C4 in the Risk Function. A steepest descent method was used to find the parameter values which gave the maximum likelihood and defined the best agreement between theory and experiment. The natural logarithm of this likelihood is -100.16, and the corresponding parameter values are

C1 = 0.6
C2 = 0.0533
C3 = 0.3457
C4 = 2.0868

The relationship between K in the rate equation and the saturation depth can now be determined for any decompression risk. The total decompression time for ascent from a saturation pressure Ps to a final pressure Pf (the surface or the pressure at which decompression sickness occurred) at a constant PIO2 is

$$t = \frac{Psat - Pf}{R} \qquad (9)$$

Substituting this and R = K * PIO2 into equation 5 and solving for K with V0 equal zero gives

$$K = \frac{C2}{C1 - \frac{V}{Psat - Pf}} \qquad (10)$$

The value of V in equation 10 corresponding to any decompression risk can be found from equation 7. Equation 10 also may be used to find the value of K for each decompression schedule.

This information is shown in Fig. 8. The curves indicate how K decreases with increasing saturation depth for decompression risks of 2, 5, 10, 20, 30, 40, 50, and 60%. The value of K for each decompression schedule is shown by a square, a diamond, or a circle. The enclosed number is the percentage of decompression sickness observed for that schedule. The square indicates that there were 2 to 6 trials on a schedule, the diamond indicates 10 to 15 trials, and the circle indicates 18 to 48 trials. The mean error between observed and predicted decompression sickness for the 21 schedules was 11%. As might be expected, the errors were greatest for schedules with the fewest trials. Table 4 lists the values of K as a function of saturation depth and decompression risks of 1, 2, and 5%.

Table 4. K as a function of saturation depth and DCS risk.

	K (FPH/ATM)			
DCS Risk	1%	2%	5%	10%
Depth (FSW)				
30	4.42	5.53	11.05	-
40	3.92	4.53	6.53	13.21
50	3.67	4.08	5.24	7.77
60	3.52	3.83	4.63	6.09
70	3.43	3.67	4.28	5.28
80	3.35	3.56	4.05	4.80
90	3.30	3.48	3.88	4.48
100	3.26	3.41	3.76	4.26
110	3.23	3.36	3.67	4.09
120	3.20	3.32	3.59	3.96
130	3.18	3.29	3.53	3.85
140	3.16	3.26	3.48	3.77
150	3.14	3.24	3.44	3.70
160	3.13	3.21	3.40	3.64
170	3.12	3.20	3.37	3.59
180	3.11	3.18	3.34	3.54
190	3.10	3.17	3.32	3.51
200	3.09	3.15	3.29	3.47

Estimation of Saturation Decompression Schedules

The dashed line in Fig. 8 is from earlier estimates of how K varies with saturation depth for both nitrogen-oxygen and helium-oxygen (Vann 1984). Maximum likelihood gives a more objective estimate of K, but it is necessary to choose a suitable decompression risk. A 2% risk was arbitrarily selected, and schedules were calculated for air decompression using the appropriate value of K for the saturation depth. These schedules are shown in Fig. 9 and are listed in Appendix B.1 (FSW) and Appendix B.2 (MSW). To avoid pulmonary oxygen exposures of greater than 600 CPTD, the maximum depth was limited to 80 FSW. The ascent rate was reduced at 10 FSW intervals to compensate for the falling oxygen partial pressure as required by the rate equation. The ascent rate was calculated for the PIO2 at the end of the depth inter-

val. For dives to 50 FSW and deeper, a PIO2 of 0.5 ATM was assumed at saturation depth, and K was reduced so that decompression could begin immediately upon switching to air without an equilibration period.

A second set of schedules (see Fig. 10, Appendix B.3 (FSW), and Appendix B.4 (MSW)) was calculated for a PIO2 of 0.5 ATM on the bottom and to 45 FSW during decompression. Air is used from 45 FSW to the surface. These schedules are not limited by pulmonary oxygen toxicity and have saturation depths ranging from 200 to 30 FSW in 10 FSW increments. The ascent rate is constant until 45 FSW after which it is reduced at 10 or 15 FSW intervals as required by the falling oxygen partial pressure.

Schedules also were calculated for a PIO2 of 0.6 ATM (see Fig. 11, Appendix B.5 (FSW), and Appendix B.6 (MSW)) which allowed a savings in decompression time of up to 10%. These schedules use a PIO2 of 0.5 ATM on the bottom and do not exceed a pulmonary oxygen exposure of 600 CPTD for decompression from the maximum depth of 170 FSW. Air is used from 60 FSW to the surface. The value of K was chosen so that decompression could begin immediately upon raising the PIO2 to 0.6 ATM. In terms of depth traveled per UPTD, oxygen is most efficiently used during decompression at partial pressures of just over 0.5 ATM.

Conclusions

This paper began by discussing an empirical method for finding the ascent rates from saturation dives. These rates were estimated in a subsequent analysis. The estimates are easily modified and can be refined with additional data and other decompression models. Perhaps

more important, however, is the likelihood principle described by Weathersby et al. (1984). This principle has at last bridged the gap between theory and experiment and may be the most significant theoretical tool in diving since Haldane's decompression model.

EVALUATION OF SATURATION DECOMPRESSION SCHEDULES BY DOPPLER METHODS

Let us now consider the evaluation of decompression schedules using precordial doppler bubble detection methods.

Doppler and Likelihood

If we define the probability of decompression sickness at each of the 5 bubble grades i = 0 to 4 as Pi(DCS), the likelihood at each grade is the probability of the observed outcome as in equation 7. For example, the likelihood at grade 2 (i = 2) is P2(DCS) if the outcome is 1 and P2(no-DCS) if the outcome is 0. For a series of observations including all bubble grades, the likelihood L can be shown to be

$$L = \prod_{i=0}^{4} \left[Pi^{Di} * (1 - Pi)^{Ni} \right] \qquad (11)$$

where Pi is the probability of decompression sickness at each grade, Di is the number of decompression incidents at each grade, and Ni is the number of safe dives at each grade. The maximum likelihood is found to occur when the probabilities are equal to the fractions of decompression sickness at each grade or

$$Pi(DCS) = \frac{Di}{Di + Ni} \qquad (12)$$

At bubble grade 3 for example, if there were 13 incidents of decompression sickness (D3 = 13), and 90 safe dives (N3 = 90), the

probability of decompression sickness is 13 divided by 103 or 12.6%.

The Relationship between Bubbles and Decompression Sickness

The probabilities of decompression sickness at all bubble grades are shown in Fig. 12 for doppler data taken from subsaturation diving, altitude exposure, and saturation diving with air or nitrogen-oxygen. The ordinate is the probability of decompression sickness as determined by equation 12, and the abcissa is the maximum bubble grade observed when the subjects flexed their limbs. The number of decompression incidents divided by the number of doppler observations at that bubble grade is shown next to each point. When decompression sickness occurred, the affected limb usually had the maximum bubble grade.

The greatest volume of data (open circles) is from subsaturation diving (Vann et al. 1982). The altitude data (crosses) were taken by NASA during tests of decompression procedures for the Shuttle (Horrigan et al. 1984). The high incidence of decompression sickness (40 cases in 173 exposures) reflects NASA's conservative attitude towards decompression sickness. Symptoms such as joint awareness, which divers would dismiss as "niggles" or "inkles", are treated by recompression to sea level.

For saturation diving (the heavy line), data on only 52 exposures could be found (Barry et al. 1984; Eckenhoff and Vann 1985). Additional data would probably reduce the apparantly high risks at grades 3 and 4 to the levels for altitude exposure and subsaturation diving. All 3 categories of data, however, exhibit the same qualitative beha-

vior in that the risk of decompression sickness increases with the bubble grade. Indeed, 71 of the 81 cases (88%) in Fig. 12 occurred at bubble grades of 3 or 4.

It is uncertain whether there is a causal relationship between precordial intravascular bubbles and the bubbles which are presumably responsible for pain-only decompression sickness. It seems more likely that the increase in decompression sickness which occurs at grades 3 and 4 is a reflection of a generally higher state of bubble formation throughout the body.

While 4 is highest grade assigned on the Spencer or similar Kisman-Masurel doppler scales, it represents saturation of the doppler signal and not the maximum gas load that can occur. Spencer and his colleagues have shown that far higher central venous gas loads are possible (Powell et al. 1982). In sheep, for example, grade 4 bubbles produce about a 20% increase in right ventricular systolic pressure. A gas load 5 times greater results in a 90% increase in RVSP. It may not be unreasonable to view the data in Fig. 12 as 5 discrete points on the left end of a dose-response curve. Gas loads to the right of grade 4 bubbles, then, would indicate an almost certain risk of decompression sickness.

The Evaluation of Individual Schedules by Doppler Monitoring

Doppler data from individual schedules is also informative. In Fig. 13, depth is shown on the left vertical axis, time on the horizontal axis, and the mean maximum doppler bubble grade on the right vertical axis. The light line is the 75 FSW SUREX decompression sche-

dule (Eckenhoff and Vann 1985), and the heavy line is the mean bubble grade. The SUREX schedule was calculated using the rate equation with K equal to 6. No bubbles were observed until 10 FSW, and the highest mean grade did not exceed 0.5. One case of decompression sickness occurred in 24 trials for an incidence of 4%. This case was associated with grade 4 bubbles.

The combined doppler data from all saturation observations shown in Fig. 12 can be used to estimate decompression risk for individual schedules by using the relationship

$$\text{Estimated DCS Risk} = \frac{\sum_{i=0}^{4} (Pi * Ti)}{\sum_{i=0}^{4} Ti} \qquad (13)$$

where Pi are the DCS probabilities at each bubble grade for all doppler data (Fig. 12), and Ti are the observations made at each grade on an individual schedule. Equation 12 predicts an 8% incidence of decompression sickness for the SUREX schedule.

Figure 14 shows the AIRSAT 4 schedule for decompression on air from 132 FSW (Eckenhoff and Vann 1985). This schedule was calculated using the rate equation with a K of 5. One case of decompression sickness occurred in 18 trials for an incidence of 6%. This diver had grade 3 bubbles. Few other divers had bubbles as indicated by the low mean bubble grade. Equation 13 predicts a 6% incidence of decompression sickness for this schedule.

Figure 15 shows the profile of the 165 FSW dive sponsored by NOAA and Oceaneering International and conducted at the F.G. Hall Laboratory of Duke University. All divers had bubble grades of at least 2. There were 5 cases of decompression sickness in 10 divers for a 50% incidence. The incidence predicted by equation 13 is 28%. It is unfortunate that doppler measurements did not begin deeper than 30 FSW so that the complete bubble profile could be studied.

Such information may prove of great value as illustrated by the ENTEX VIII decompression schedule (Fig. 16) which was used after a 450 MSW helium-oxygen dive (Masurel 1984). Each point in Fig. 16 is the mean of 12 doppler measurements per day taken on 4 divers. The mean bubble grade increased steadily to 2.5 during the first phase of decompression and did not decline until the rate of ascent was reduced. Decompression sickness did not occur, and the mean grade upon surfacing was low. Yet, given the damage which free gas can cause in blood (Hallenbeck and Andersen 1982), one must wonder at the advisability of maintaining a steady flow of bubbles over a period of several days. While little damage probably occurs at the low gas loads involved, the unnecessary risk could easily be eliminated by reducing the initial rate of ascent.

Conclusions

This brief review of doppler bubble measurements suggests several conclusions. First, the relationship between bubbles and decompression sickness is qualitatively similar for a variety of decompression exposures. Second, most decompression sickness is associated with high

bubble grades. Third, doppler bubble detectors can monitor the progressive development of bubbles during a saturation decompression, and the extent of these bubbles can be reduced by decreasing the rate of ascent.

A final conclusion relates to the purpose of this workshop. Likelihood and doppler bubble detection methods are powerful theoretical and experimental tools for solving the problems of decompression. If these tools are to be used effectively, however, adequate support for research must be available and sufficient data from experimental and operational diving must be accurately recorded and published for general use.

References

Barry, P.D., R.D. Vann, D.A. Youngblood, R.E. Peterson, and P.B. Bennett. 1984. Decompression from a deep nitrogen/oxygen saturation dive: a case report. Undersea Biomed. Res. 11(4): 387-393.

Eckenoff, R.G. and R.D. Vann. 1985. Air and nitrogen/oxygen saturation decompression: a report of 4 schedules and 77 subjects. Undersea Biomed. Res. 12(5): In press.

Hamilton, R.W., Adams, G.M., Harvey, C.A., and Knight, D.R. (eds.) SHAD-NISAT: a composite study of simulated shallow saturation diving. Naval Submarine Medical Research Laboratory Report Number 985. August 1982.

Horrigan, D.J., Jr., J.M. Waligora, A.T. Hadley III, and J. Conkin. 1984. Doppler measurements of intravenous gas bubbles during 6 hours of exercise at space suit pressures. Aerospace Medical Assn. Scientific Program. May 6-10. San Diego.

Masurel, M.G. 1984. Detection ultra sonore de bulles circulantes. Chap. 9 in ENTEX VIII: experience de plongee fictive profonde a 46 ATA (450 m) avec 12 jours de sejour au fond et travail en position immergee. Rapport final du contract D.R.E.T./Marine Nationale 81/1281. Direction des Recherches et Etudes Techniques. Ed. B. Broussolle. C.E.P. Ismer, B.P. 5 83800, Toulon/Naval, France

Miller, J.W. (ed.) 1976. Vertical Excursions Breathing Air from Nitrogen-Oxygen or Air Saturation Exposures. U.S. Department of Commerce, Rockville, Md. May 1976.

Muren, A., J. Adolfson, H. Ornhagen, M. Gennser, and R.W. Hamilton. 1984. NISAHEX: Deep nitrox saturation with nitrox and trimix excursions. In: Underwater Physiology VIII. Eds. A.J. Bachrach and M.M. Matzen. Pp. 713-730.

Philp, R.B., P.B. Bennett, J.C. Andersen, G.N. Fields, B.A. McIntyre, I. Francey, and W. Briner. 1979. Effects of asprin and dipyridamole on platelet function, hematology, and blood chemistry of saturation divers. Undersea Biomed. Res. 6(2): 127-145.

Powell, M.R., M.P. Spencer, and O.T. von Ramm. 1982. Ultrasonic surveillance of decompression. In: The physiology of diving and compressed air work, 3rd edn., pp.404-434. Ed.P.B.Bennett and D.H.Elliott. London: Bailliere Tindall.

Schreiner,H.R. and P.L.Kelley. 1967. Computation methods for decompression from deep dives. In: Proc. 3rd Symp. Underwater Physiol. Ed. C.J. Lambertsen. Pp. 277-299. Baltimore: Williams and Wilkins.

Thalmann, E.D. 1984. Development of a 60 FSW air saturation decompression schedule. Undersea Biomed. Res. 11 (1, Suppl.): Abstract 18.

Van Liew, H.D., B. Bishop, D. Walder, and H. Rahn. 1965. Effects of compression on composition and absorption of tissue gas pockets. J. Appl. Physiol. 20: 927-933.

Van Liew, H.D., W.H. Schoenfisch, and A.J. Olszowka. 1968. Exchanges of N2 betewwn a gas pocket and tissue in a hyperbaric environment. Resp. Physiol. 6: 23-28.

Vann, R.D. 1984. Decompression after saturation diving. In: Proceedings of the 3rd Annual Canadian Ocean Technology Congress. March 21-23. Toronto. Pp. 175-188.

Vann, R.D., A.P. Dick, and P.D. Barry. 1982. Doppler bubble measurements and decompression sickness. Undersea Biomed. Res. 9(1, Suppl.): 24.

Vorosmarti, J., R. de G. Hanson, and E.E.P. Barnard. 1978. Decompression from steady-state exposures to 250 meters. In: Underwater Physiology VI, pp. 435-442. Eds. C.W. Shilling and M.W. Beckett. Bethesda, MD: FASEB.

Weathersby, P.K., L.D. Homer, and E.T. Flynn. 1984. On the liklihood of decompression sickness. J. Appl. Physiol.: Respirat. Environ. Exercise Physiol. 57(3): 815-825.

Workman, R.D. 1969. American decompression theory and practice. In: The physiology and medicine of diving and compressed air work, 1st edn, pp. 252-290. Eds. P.B. Bennett and D.H. Elliott. London: Bailliere, Tindall, and Cassell.

Appendix A. N2-O2 saturation decompression schedule data.

INITIAL DEPTH (FSW)	FINAL DEPTH (FSW)	FIO2	PIO2 (ATM)	TIME (HR)	DCS	DIVES	REFERENCE
50.	20.	.21	.0	3.0			
20.	10.	.21	.0	2.5			
10.	5.	.21	.0	1.67			PRE-SHAD
5.	0.	.21	.0	2.5	2.	2.	HAMILTON ET AL (1982)
50.	35.	.21	.0	1.5			
35.	10.	.21	.0	6.25			
10.	5.	.21	.0	2.75			SHAD I
5.	0.	.21	.0	3.	0.	2.	HAMILTON ET AL (1982)
50.	35.	.21	.0	2.5			
35.	21.	.21	.0	3.5			SHAD III
21.	18.	.21	.0	2.7	1.	3.	HAMILTON ET AL (1982)
60.	45.	.21	.0	2.5			
45.	19.	.21	.0	6.5			SHAD II
19.	12.	.21	.0	3.85	1.	2.	HAMILTON DT AL (1982)
60.	30.	.21	.0	3.0			
30.	28.	.21	.0	0.73			
28.	26.	.21	.0	0.77			
26.	24.	.21	.0	0.8			
24.	22.	.21	.0	0.83			
22.	20.	.21	.0	0.87			
20.	18.	.21	.0	0.9			
18.	16.	.21	.0	0.93			
16.	13.	.21	.0	1.45			
13.	10.	.21	.0	1.5			
10.	8.	.21	.0	1.03			
8.	6.	.21	.0	1.07			
6.	4.	.21	.0	1.1			SCORE
4.	2.	.21	.0	1.13			MILLER (1976)
2.	0.	.21	.0	1.13	7.	48.	PHILP ET AL (1979)
60.	50.	.18	.0	2.5			
50.	33.5	.18	.0	5.5			
33.5	33.5	.18	.0	2.			DIVE 1
33.5	0.	.18	.0	11.17	4.	10.	THALMANN (1984)
60.	50.	.21	.0	2.5			
50.	39.5	.21	.0	3.5			
39.5	39.5	.21	.0	6.			
39.5	15.5	.21	.0	8.			
15.5	15.5	.21	.0	2.			DIVE 2
15.5	0.	.21	.0	5.17	3.	10.	THALMANN (1984)
60.	50.	.21	.0	0.01			
50.	26.	.21	.0	8.			
26.	26.	.21	.0	4.			
26.	12.	.21	.0	4.			
12.	12.	.21	.0	8.			DIVE 3
12.	0.	.21	.0	3.	1.	10.	THALMANN (1984)

Appendix A. (Continued)

INITIAL DEPTH (FSW)	FINAL DEPTH (FSW)	FIO2	PIO2 (ATM)	TIME (HR)	DCS	DIVES	REFERENCE
60.	40.	.21	.0	0.01			
40.	30.	.21	.0	3.33			DIVE 4
30.	14.	.21	.0	8.	1.	10.	THALMANN (1984)
60.	40.	.18	.0	0.01			
40.	40.	.18	.0	4.33			
40.	30.	.18	.0	3.33			
30.	10.	.18	.0	10.			DIVE 5
10.	0.	.18	.0	10.	1.	11.	THALMANN (1984)
60.	30.	.18	.0	10.			
30.	10.	.18	.0	10.			DIVES 6 & 7
10.	0.	.18	.0	10.	1.	20.	THALMANN (1984)
60.	40.	.18	.0	6.67			
40.	20.	.18	.0	10.			DIVE 8
20.	0.	.18	.0	20.	0.	10.	THALMANN (1984)
60.	45.	.21	.0	2.5			
45.	20.	.21	.0	6.25			
20.	5.	.21	.0	8.25			AIRSAT 1 & 2
5.	0.	.21	.0	3.0	2.	23.	ECKENHOFF AND VANN (1984)
65.	60.	.21	.0	1.42			
60.	50.	.21	.0	3.17			
50.	40.	.21	.0	3.67			
40.	30.	.21	.0	4.17			
30.	20.	.21	.0	5.0			
20.	10.	.21	.0	6.17			SUREX 65
10.	0.	.21	.0	8.0	1.	18.	ECKENHOFF AND VANN (1984)
75.	70.	.21	.0	1.33			
70.	60.	.21	.0	2.83			
60.	50.	.21	.0	3.17			
50.	40.	.21	.0	3.67			
40.	30.	.21	.0	4.17			
30.	20.	.21	.0	5.0			
20.	10.	.21	.0	6.17			SUREX 75
10.	0.	.21	.0	8.0	0.	6.	ECKENHOFF AND VANN (1984)
90.	60.	.095	.0	3.0			
60.	40.	.19	.0	5.0			
40.	30.	.21	.0	2.5			
30.	20.	.21	.0	3.33			
20.	10.	.21	.0	4.17			NOAA OPS I
10.	0.	.21	.0	5.0	0.	3.	MILLER (1976)

Appendix A. (Continued)

INITIAL DEPTH (FSW)	FINAL DEPTH (FSW)	FIO2	PIO2 (ATM)	TIME (HR)	DCS	DIVES	REFERENCE
132.	112.	.21	.0	4.0			
112.	112.	.21	.0	2.0			
112.	100.	.21	.0	2.4			
100.	77.6	.21	.0	5.6			
77.6	77.6	.21	.0	6.0			
77.6	50.	.21	.0	6.9			
50.	46.7	.21	.0	1.1			
46.7	46.7	.21	.0	2.0			
46.7	22.7	.21	.0	8.0			
22.7	22.7	.21	.0	6.0			AIRSAT 3
22.7	0.	.21	.0	7.57	3.	12.	ECKENHOFF AND VANN (1984)
132.	50.	.0	.5	32.8			
50.	40.	.21	.0	4.33			
40.	30.	.21	.0	5.0			
30.	20.	.21	.0	6.0			
20.	10.	.21	.0	7.33			AIRSAT 4
10.	0.	.21	.0	9.67	1.	15.	ECKENHOFF AND VANN (1984)
165.	115.	.0	.5	13.5			
115.	60.	.0	.5	27.83			
60.	45.	.0	.5	9.58			OI/NOAA/DUKE
45.	20.	.21	.0	14.26	5.	10.	BARRY ET AL (1984)
197.	184.	.0	.5	1.0			
184.	66.	.0	.5	36.0			
66.	45.	.0	.5	12.57			NISAHEX
45.	36.	.21	.0	5.43	5.	6.	MUREN ET AL (1984)
198.	188.	.0	.3	1.67			
188.	177.	.0	.3	2.75			
177.	14.	.0	.3	143.98			NISAT I
14.	0.	.21	.0	12.6	0.	3.	HAMILTON ET AL (1982)

Appendix B.1 Air saturation decompression schedules in FSW. At saturation depths of 45 FSW or shallower, air is used. At saturation depths greater than 45 FSW, a PIO2 of 0.5 ATM is used. Decompression can begin immediately after raising the oxygen level to 21%. Pulmonary oxygen exposures do not exceed 600 CPTD.

SATURATION DEPTH, FSW	RATE OF ASCENT, MIN/FSW, IN DEPTH RANGE								DECOMPRESSION TIME		
	80 TO 70	70 TO 60	60 TO 50	50 TO 40	40 TO 30	30 TO 20	20 TO 10	10 TO 0	DAY	HR	MIN
30						33	40	52		20	50
30 - 40					34	40	49	64	1	7	10
40 - 50				32	37	44	54	71	1	15	40
50 - 60			31	36	41	49	60	78	2	1	10
60 - 70		29	32	37	43	50	62	81	2	7	40
70 - 80	27	30	33	38	44	52	64	83	2	13	50

Appendix B.2 Air saturation decompression schedules in MSW. At saturation depths of 14 FSW or shallower, air is used. At saturation depths greater than 14 MSW, a PIO2 of 0.5 ATM is used. Decompression can begin immediately after raising the oxygen level to 21%. Pulmonary oxygen exposures do not exceed 600 CPTD.

SATURATION DEPTH, MSW	RATE OF ASCENT, MIN/(.5 MSW), IN DEPTH RANGE								DECOMPRESSION TIME		
	24 TO 21	21 TO 18	18 TO 15	15 TO 12	12 TO 9	9 TO 6	6 TO 3	3 TO 0	DAY	HR	MIN
9						53	66	85		20	24
9 - 12					55	65	80	104	1	6	24
12 - 15				52	61	72	89	115	1	7	54
15 - 18			51	58	67	80	99	128	2		18
18 - 21		47	53	60	69	82	102	132	2	6	30
21 - 24	44	48	54	61	71	84	104	135	2	12	6

Appendix B.3 N2-O2 saturation decompression schedules in FSW for 0.5 ATM PIO2. The PIO2 at saturation depth is 0.5 ATM. From 45 FSW to the surface, maintain 21% oxygen.

SATURATION DEPTH, FSW	RATE OF ASCENT, MIN/FSW, IN DEPTH RANGE					DECOMPRESSION TIME		
	TO 45	45 TO 30	30 TO 20	20 TO 10	10 TO 0	DAY	HR	MIN
30			33	40	52		20	50
30 - 40		34	40	49	64	1	7	10
40 - 50	30	37	44	54	71	1	15	55
50 - 60	32	40	47	58	75	2	0	0
60 - 70	33	41	49	60	78	2	7	10
70 - 80	34	43	50	62	81	2	14	45
80 - 90	35	44	52	64	83	2	22	25
90 - 100	36	44	53	65	84	3	5	40
100 - 110	36	45	53	66	86	3	12	25
110 - 120	37	46	54	67	87	3	20	25
120 - 130	37	46	55	67	87	4	2	45
130 - 140	37	46	55	68	88	4	9	15
140 - 150	38	47	55	68	89	4	17	35
150 - 160	38	47	56	69	90	5	0	25
160 - 170	38	47	56	69	90	5	6	45
170 - 180	38	48	56	69	90	5	13	20
180 - 190	38	48	57	70	91	5	20	10
190 - 200	39	48	57	70	91	6	5	5

Appendix B.4 N2-O2 saturation decompression schedules in MSW for 0.5 ATM PIO2. The PIO2 at saturation depth is 0.5 ATM. From 14 MSW to the surface, maintain 21% oxygen.

SATURATION DEPTH, MSW	RATE OF ASCENT, MIN/(.5 MSW) IN DEPTH RANGE					DECOMPRESSION TIME		
	TO 14	14 TO 9	9 TO 6	6 TO 3	0 TO 0	DAY	HR	MIN
9			53	66	85		20	24
9 - 12		55	65	80	104	1	6	24
12 - 15	49	61	72	89	115	1	15	24
15 - 18	52	65	77	94	123	1	23	10
18 - 21	54	67	80	99	128	2	6	28
21 - 24	56	69	82	102	132	2	13	46
24 - 27	57	71	84	104	135	2	20	50
27 - 30	58	72	86	106	138	3	3	56
30 - 34	59	74	87	108	140	3	13	10
34 - 37	60	74	88	109	142	3	20	14
37 - 40	60	75	89	110	143	4	2	42
40 - 43	61	76	90	111	144	4	10	8
43 - 46	61	76	91	112	145	4	16	32
46 - 49	62	77	91	113	147	5	0	16
49 - 52	62	77	92	113	147	5	6	34
52 - 55	62	78	92	114	148	5	13	8
55 - 58	63	78	93	114	148	5	20	54
58 - 61	63	78	93	115	149	6	3	24

Appendix B.5 N2-O2 saturation decompression schedules in FSW for 0.6 ATM PIO2. The PIO2 at saturation depth is 0.5 ATM. Decompression can begin immediately after raising the PIO2 to 0.6 ATM. From 60 FSW to the surface, maintain 21% oxygen. Pulmonary oxygen exposures do not exceed 600 CPTD.

SATURATION DEPTH, FSW	RATE OF ASCENT, MIN/FSW, IN DEPTH RANGE							DECOMPRESSION TIME		
	TO 60	60 TO 50	50 TO 40	40 TO 30	30 TO 20	20 TO 10	10 TO 0	DAY	HR	MIN
70 - 80	29	33	38	44	52	64	83	2	14	
80 - 90	30	34	38	44	53	65	84	2	20	
90 - 100	30	34	39	45	53	66	86	3	1	50
100 - 110	31	35	39	46	54	67	87	3	8	30
110 - 120	31	35	40	46	55	67	87	3	14	
120 - 130	31	35	40	46	55	68	88	3	19	30
130 - 140	31	36	40	47	55	68	89	4	1	10
140 - 150	32	36	41	47	56	69	90	4	8	30
150 - 160	32	36	41	47	56	69	90	4	13	50
160 - 170	32	36	41	48	56	69	90	4	19	20

Appendix B.6 N2-O2 saturation decompression schedules in MSW for 0.6 ATM PIO2. The PIO2 at saturation depth is 0.5 ATM. Decompression can begin immediately after raising the PIO2 to 0.6 ATM. From 18 MSW to the surface, maintain 21% oxygen. Pulmonary oxygen exposures do not exceed 600 CPTD.

SATURATION DEPTH, MSW	RATE OF ASCENT, MIN/(.5 MSW) IN DEPTH RANGE							DECOMPRESSION TIME		
	TO 18	18 TO 15	15 TO 12	12 TO 9	9 TO 6	6 TO 3	3 TO 0	DAY	HR	MIN
21 - 24	48	54	61	71	84	104	135	2	12	30
24 - 27	49	55	63	72	86	106	138	2	18	42
27 - 30	49	56	64	74	87	108	140	3		30
30 - 34	50	57	64	74	88	109	142	3	8	4
34 - 37	50	57	65	75	89	110	143	3	13	34
37 - 40	51	58	65	76	90	111	144	3	19	48
40 - 43	51	58	66	76	91	112	145	4	1	18
43 - 46	52	59	67	77	91	113	147	4	7	56
46 - 49	52	59	67	77	92	113	147	4	13	14
49 - 52	52	59	67	78	92	114	148	4	18	44

Figure Captions

1. An empirical method for developing saturation decompression schedules.
2. Saturation decompression schedules based upon the rate equation for constant PIO2 and constant FIO2.
3. The effect of saturation depth upon the bubble volume at sea level.
4. The effects of ascent rate and PIO2 upon bubble volume at sea level. Schedule 1 has a slower ascent rate than Schedule 2. Schedule 3 has a higher PIO2 and a faster ascent rate than Schedule 2.
5. A decompression model which assumes that bubble growth is proportional to the ascent rate and bubble resolution is proportional to the PIO2.
6. Bubble growth during the SCORE decompression schedule.
7. A dose-response curve relating the risk of decompression sickness to the bubble volume.
8. The relationship between the value of K in the rate equation and the saturation depth for several decompression risks. The values of K for the individual schedules are shown.
9. Saturation decompression schedules using air (see Appendices B.1 and B.2).
10. Saturation decompression schedules for a PIO2 of 0.5 ATM (see Appendices B.3 and B.4).
11. Saturation decompression schedules for a PIO2 of 0.6 ATM (see Appendices B.5 and B.6).
12. Precordial doppler bubble data for decompression after sub-saturation diving, altitude exposure, and saturation diving.
13. Mean doppler bubble grade during the SUREX decompression.
14. Mean doppler bubble grade during the AIRSAT 4 decompression.
15. Mean doppler bubble grade during the NOAA/OI decompression.
16. Mean doppler bubble grade during the ENTEX VIII decompression.

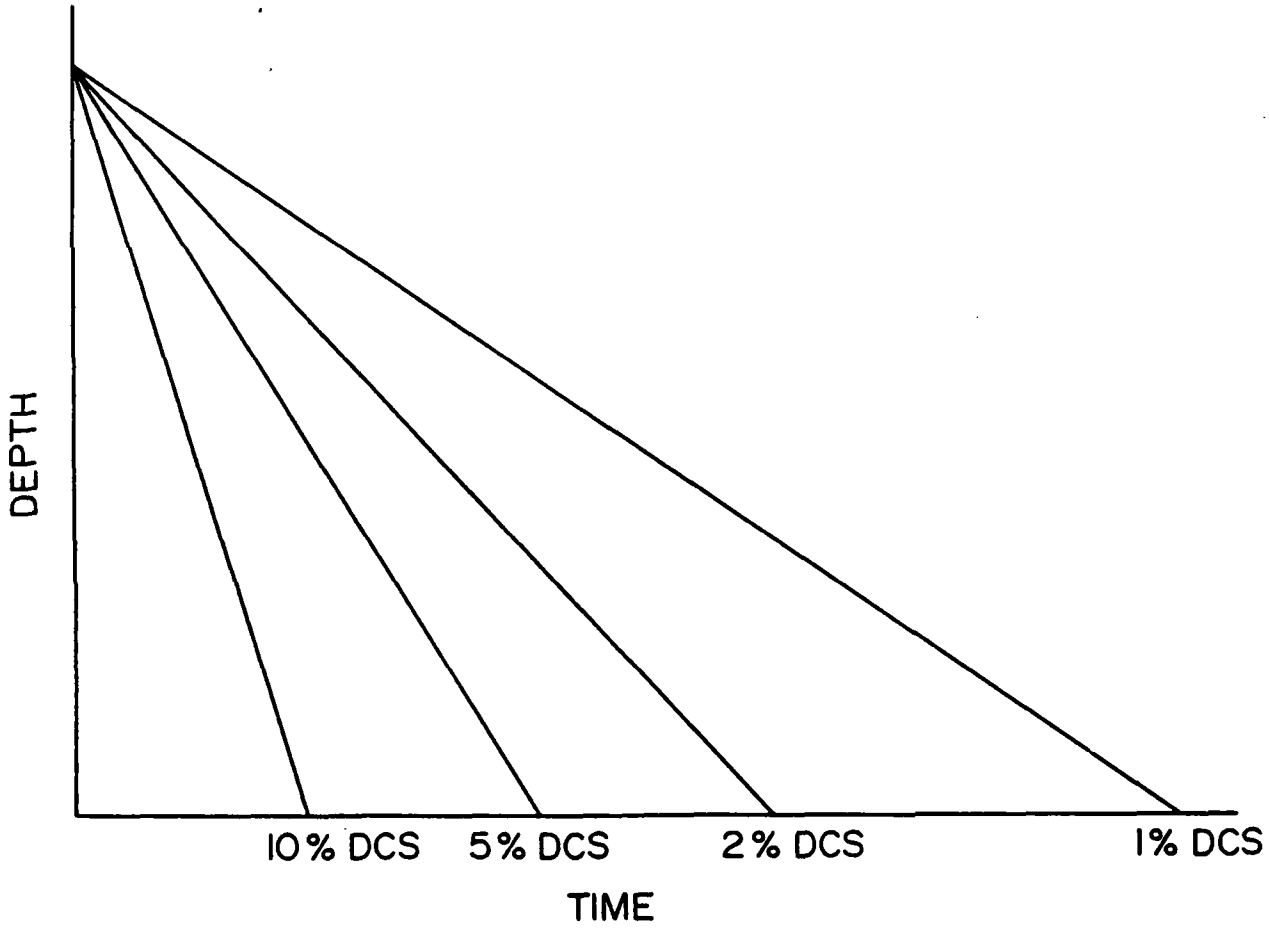
DEPTH
10% DCS
5% DCS
2% DCS
1% DCS
TIME

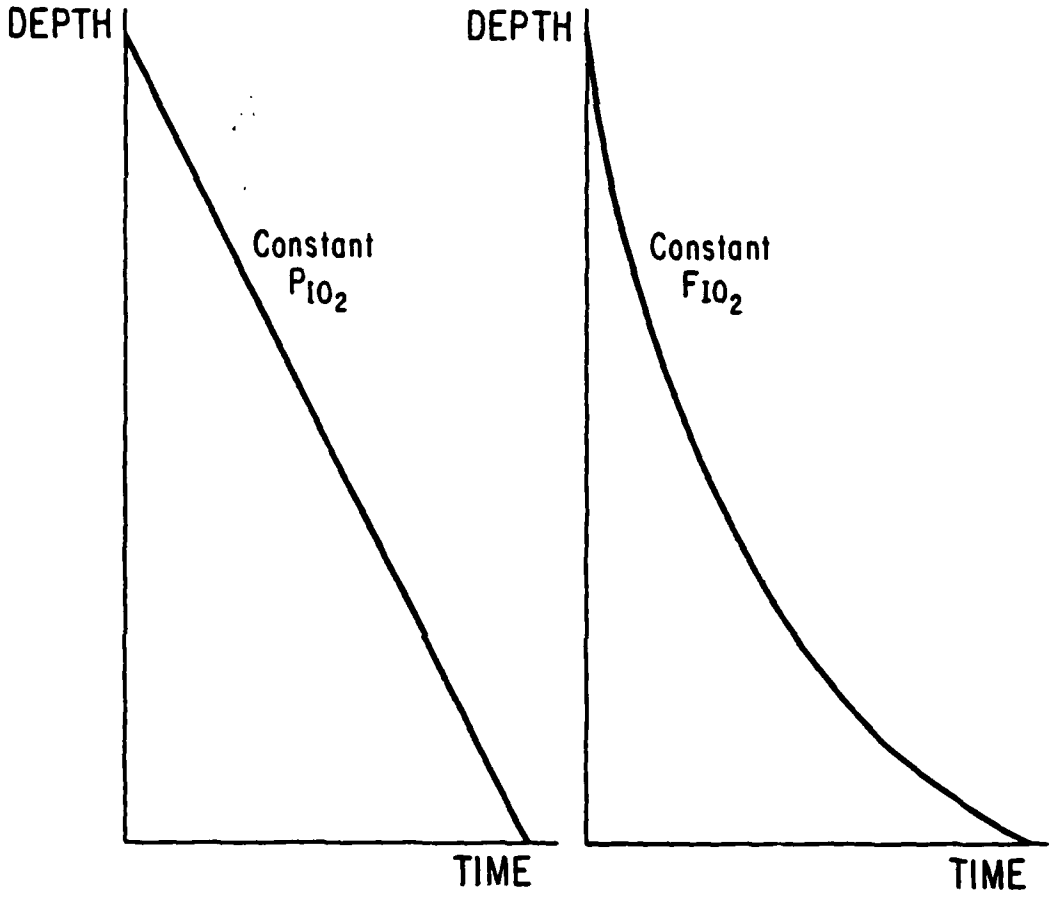
DEPTH
Constant
P_{IO_2}
TIME
DEPTH
Constant
F_{IO_2}
TIME

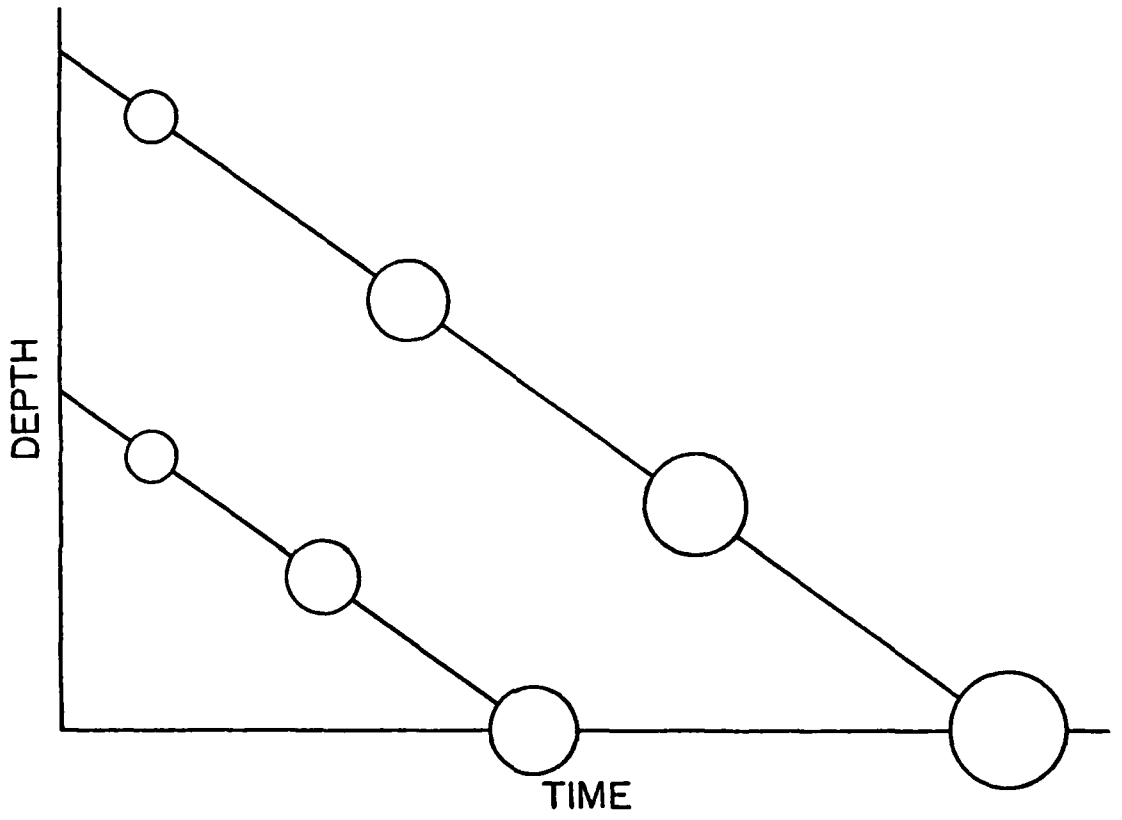
DEPTH
TIME

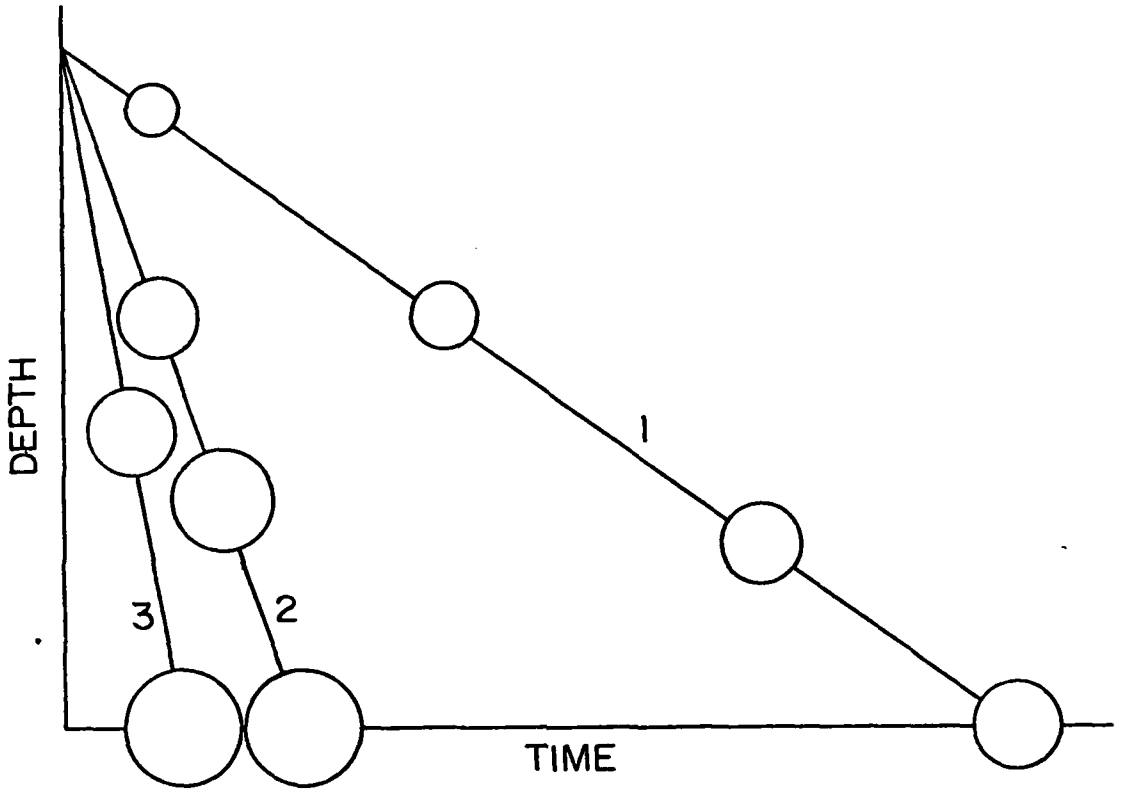
DEPTH
TIME
1
2
3

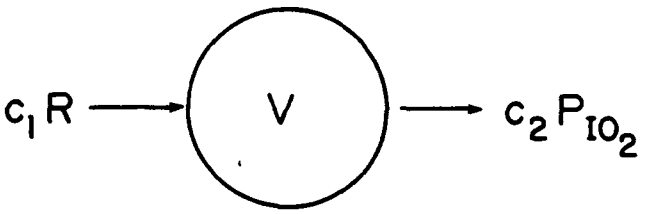

$$\dot{V} = c_1 R - c_2 P_{IO_2}$$

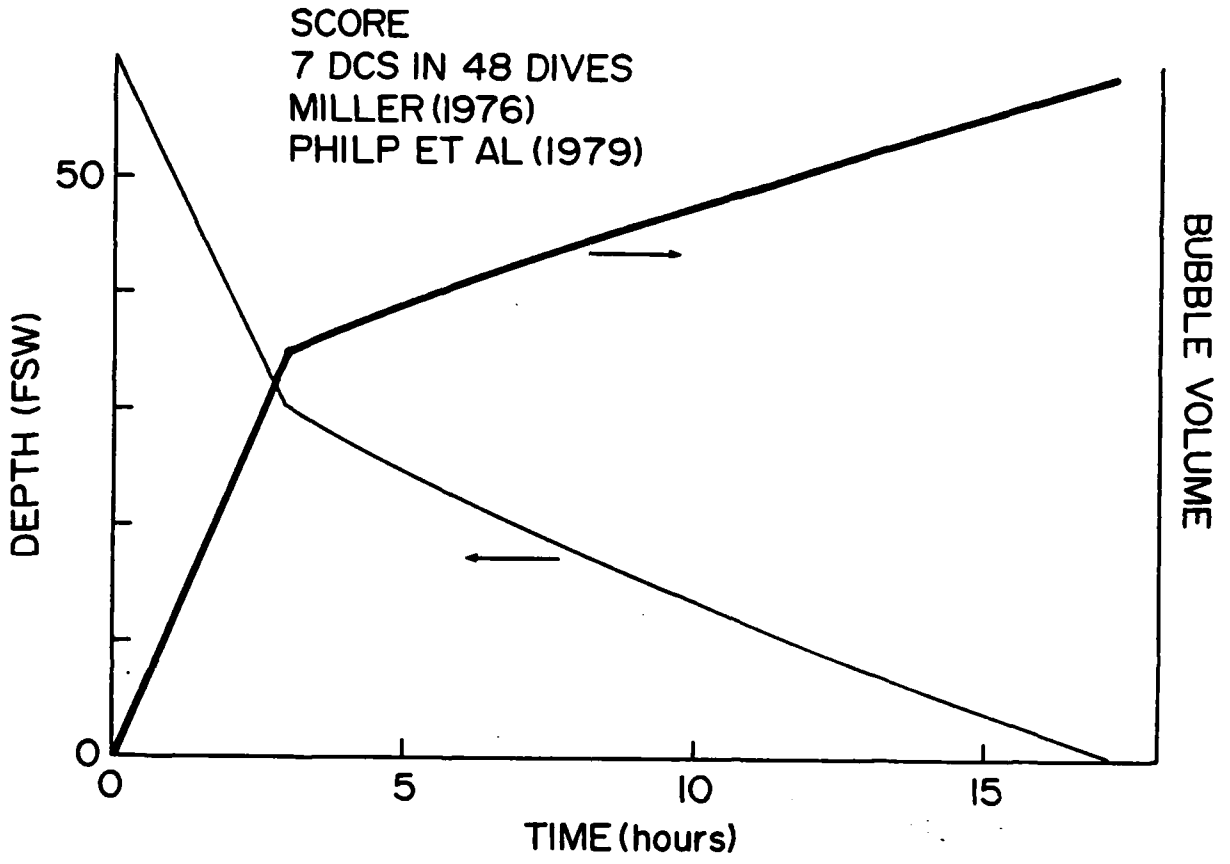
SCORE
7 DCS IN 48 DIVES
MILLER (1976)
PHILP ET AL (1979)
50
0
DEPTH (FSW)
BUBBLE VOLUME
0
5
10
15
TIME (hours)

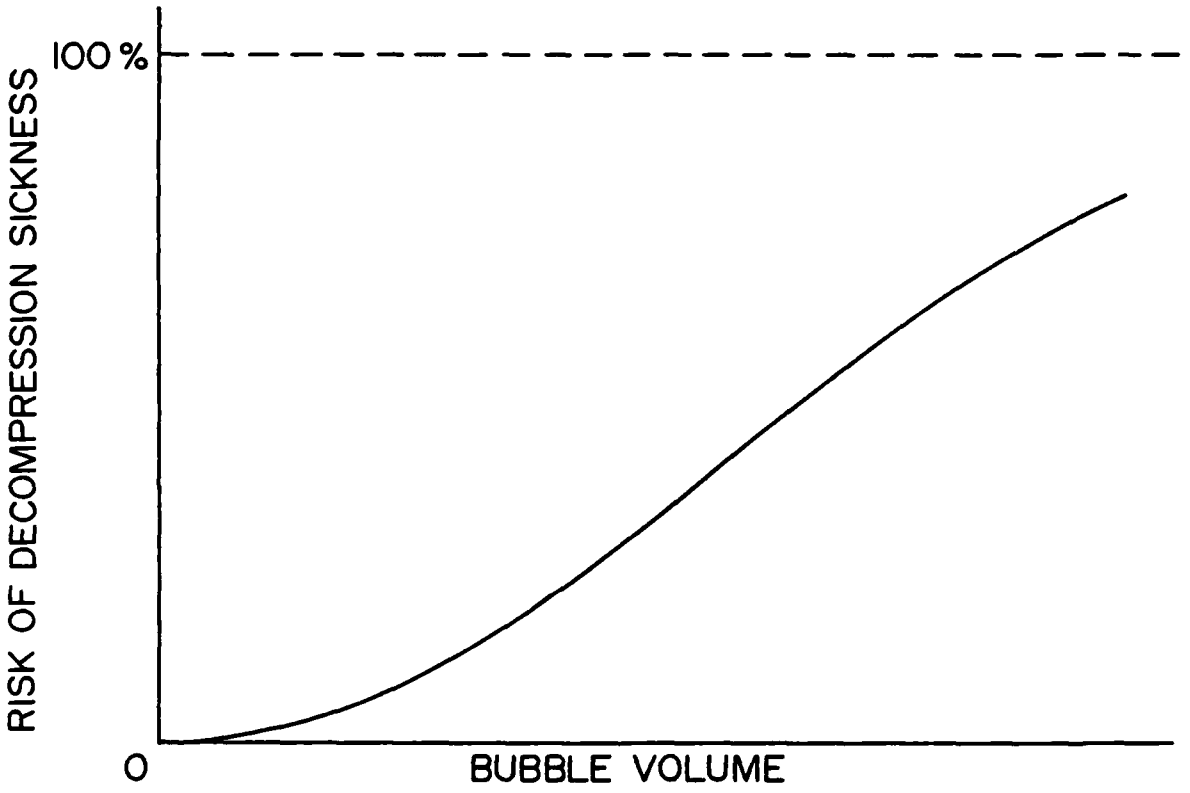
100 %
RISK OF DECOMPRESSION SICKNESS
0
BUBBLE VOLUME

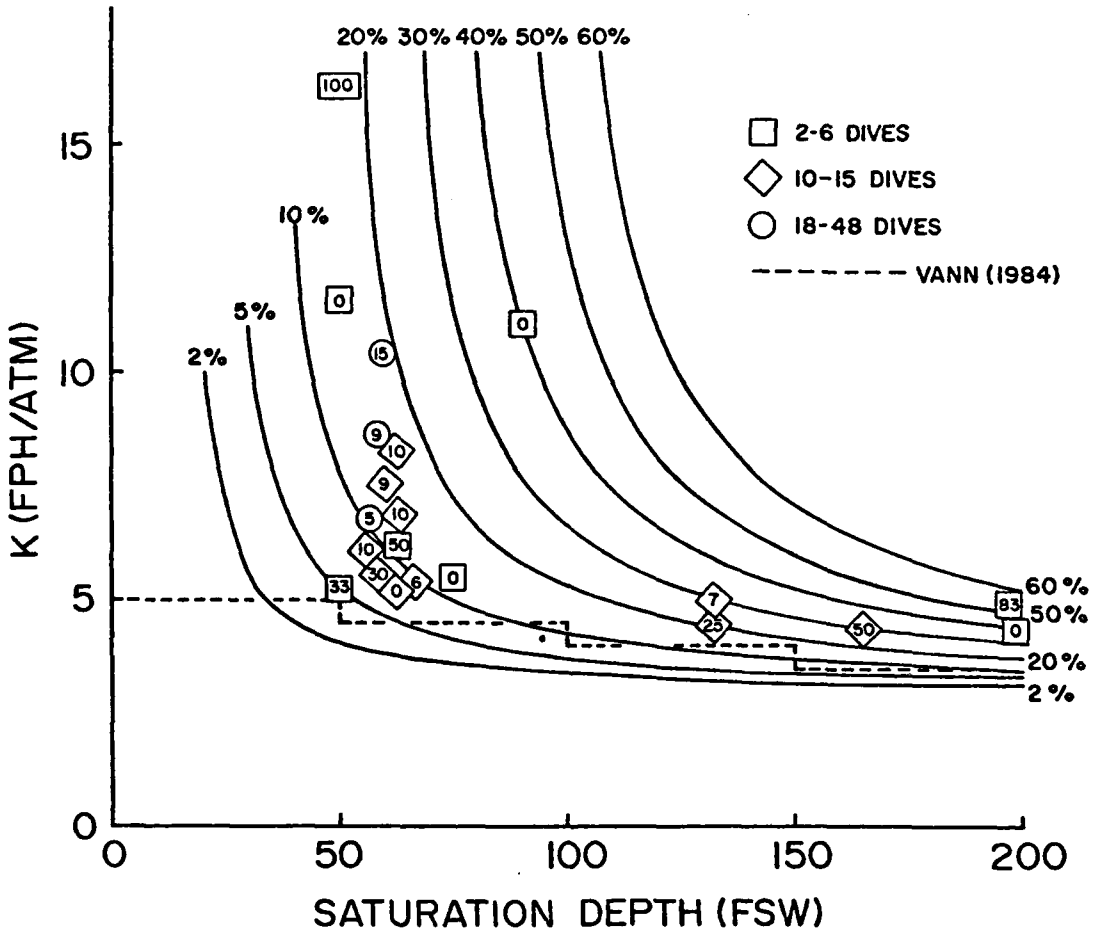
20% 30% 40% 50% 60%
2-6 DIVES
10-15 DIVES
18-48 DIVES
VANN (1984)
10%
5%
2%
60%
50%
20%
2%
K (FPH/ATM)
SATURATION DEPTH (FSW)
0
5
10
15
0
50
100
150
200

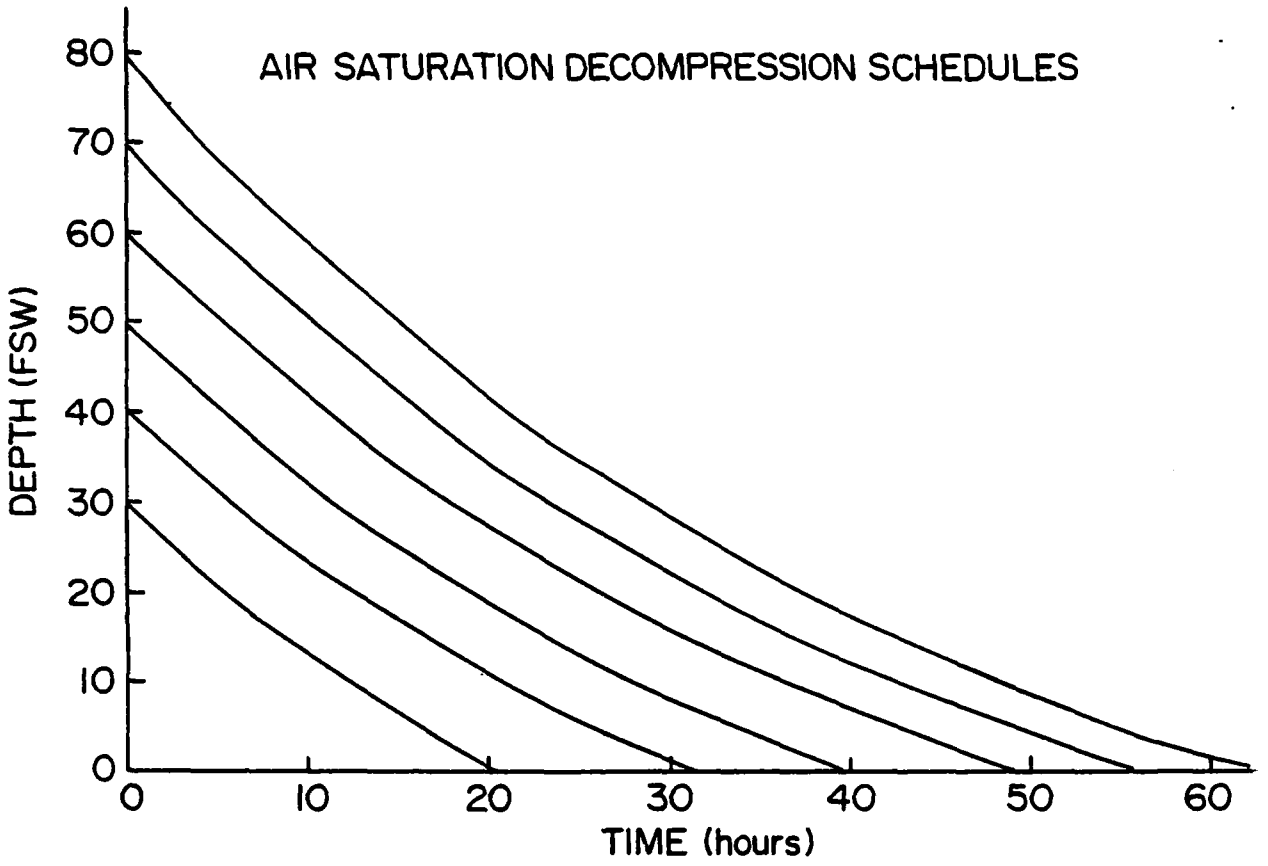
AIR SATURATION DECOMPRESSION SCHEDULES
DEPTH (FSW)
80
70
60
50
40
30
20
10
0
0
10
20
30
40
50
60
TIME (hours)

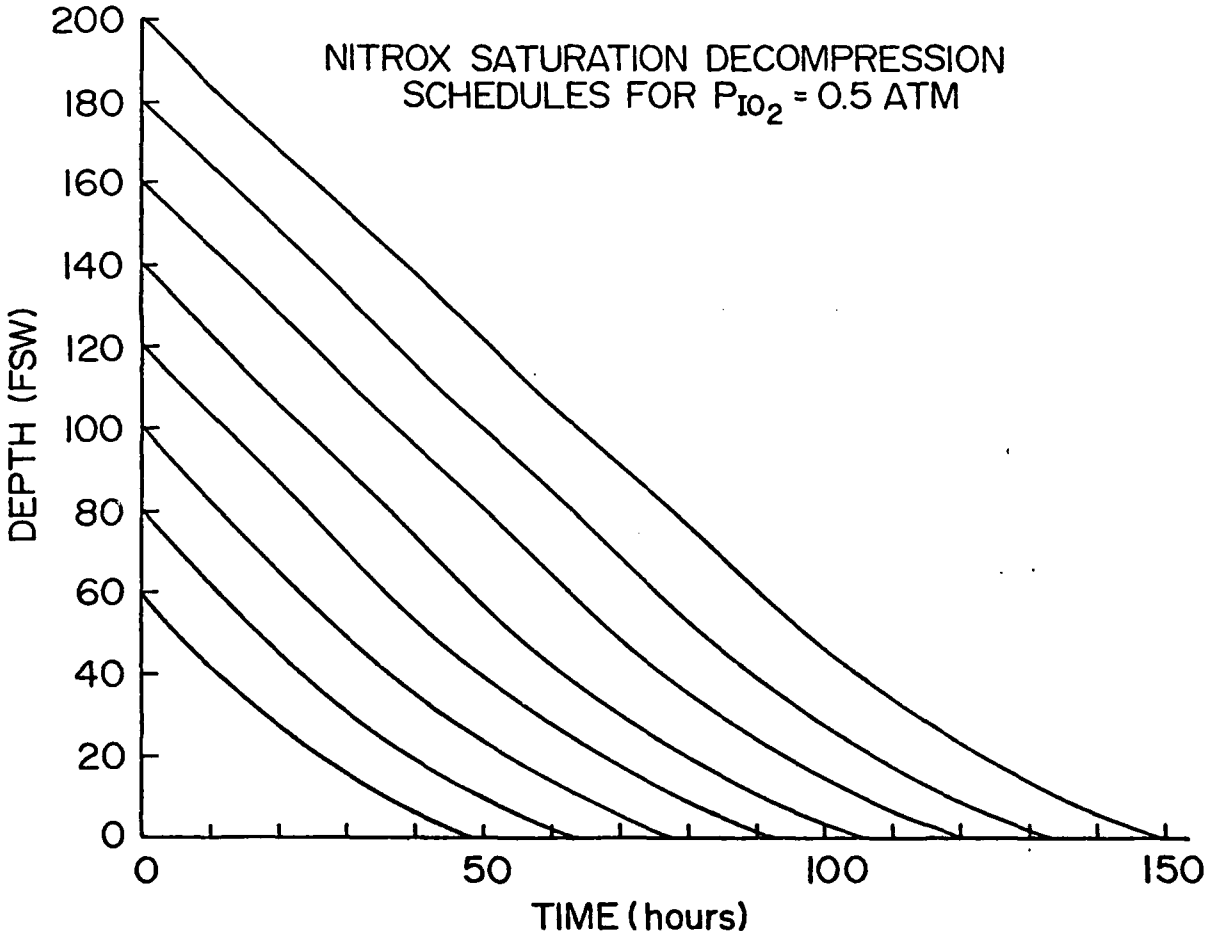
NITROX SATURATION DECOMPRESSION
SCHEDULES FOR P_{IO_2} = 0.5 ATM
DEPTH (FSW)
200
180
160
140
120
100
80
60
40
20
0
0
50
100
150
TIME (hours)

NITROX SATURATION DECOMPRESSION SCHEDULES
FOR P_{IO_2} = 0.5 AND 0.6 ATM

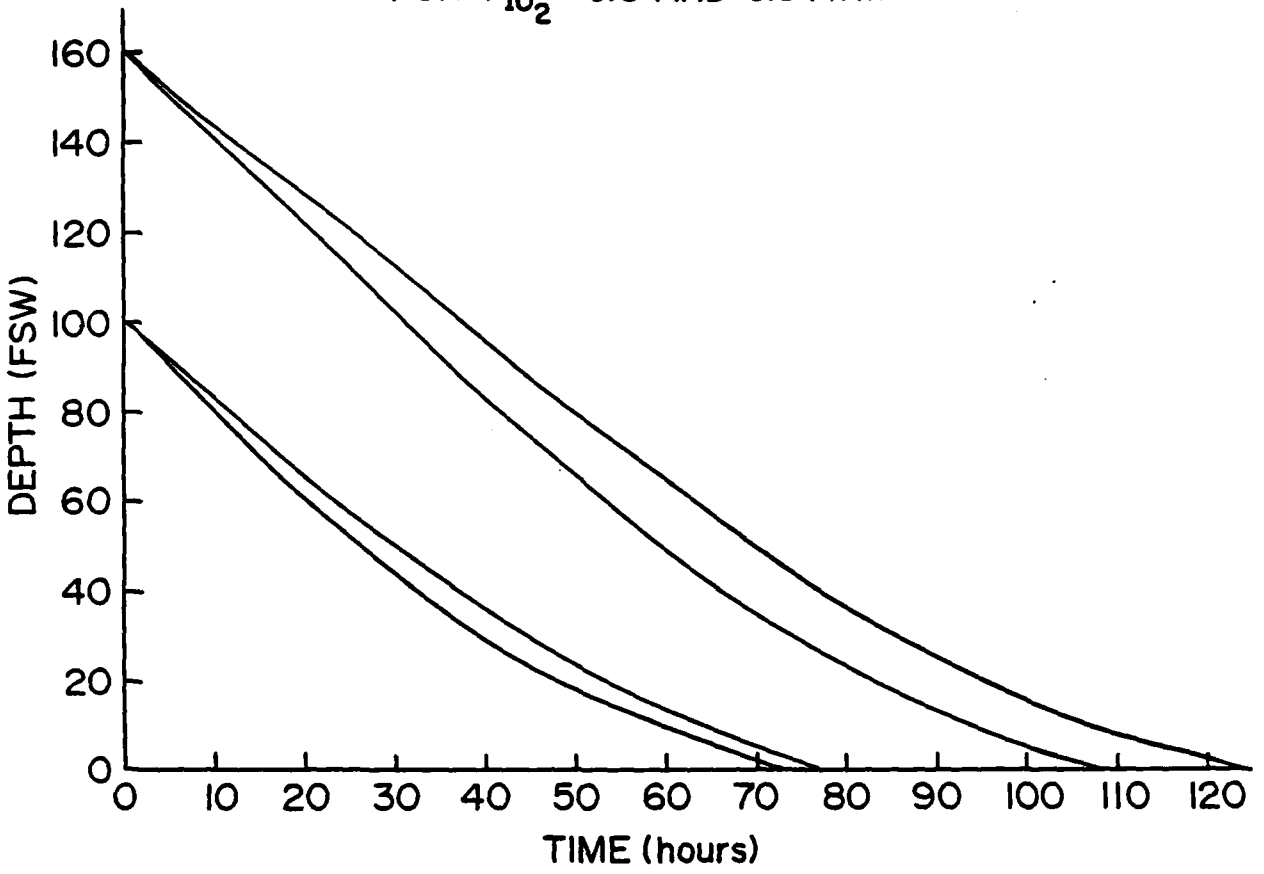

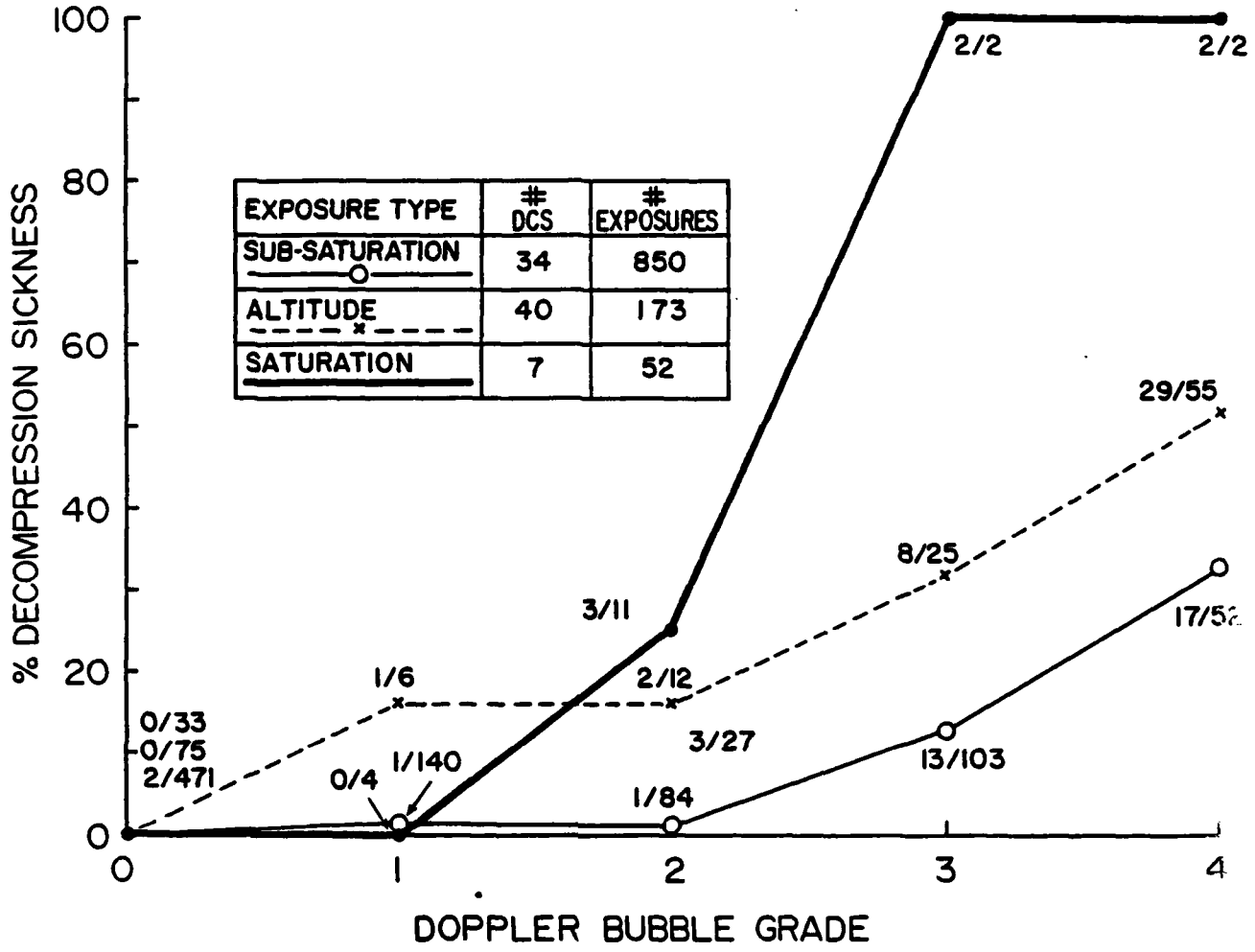
100
80
60
40
20
0
% DECOMPRESSION SICKNESS
0
1
2
3
4
DOPPLER BUBBLE GRADE
EXPOSURE TYPE
DCS
EXPOSURES
SUB-SATURATION
34
850
ALTITUDE
40
173
SATURATION
7
52
2/2
2/2
29/55
8/25
3/11
17/52
1/6
2/12
0/33
0/75
2/471
3/27
0/4
1/140
13/103
1/84

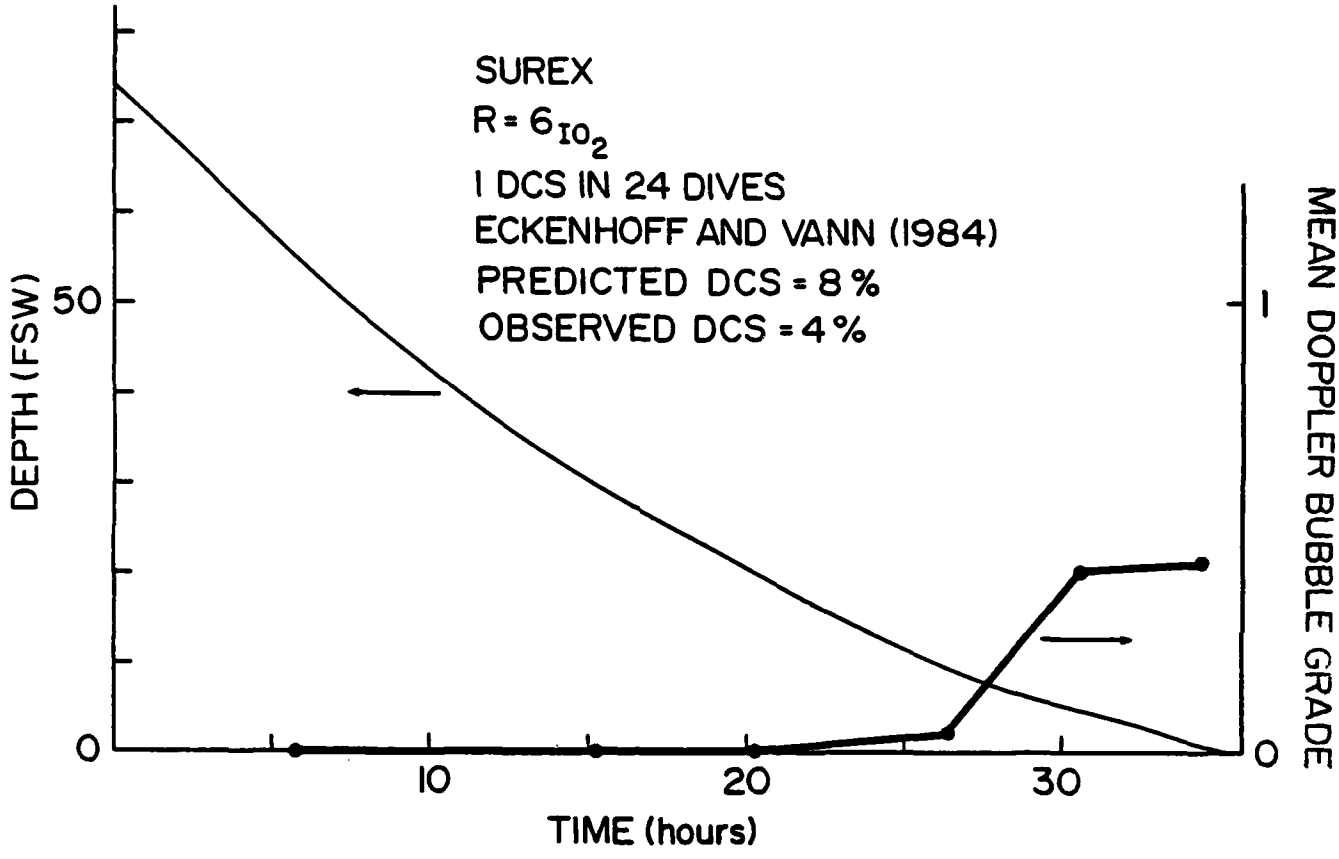
SUREX
R = 6 IO2
1 DCS IN 24 DIVES
ECKENHOFF AND VANN (1984)
PREDICTED DCS = 8 %
OBSERVED DCS = 4 %
DEPTH (FSW)
50
0
10
20
30
TIME (hours)
1
0
MEAN DOPPLER BUBBLE GRADE

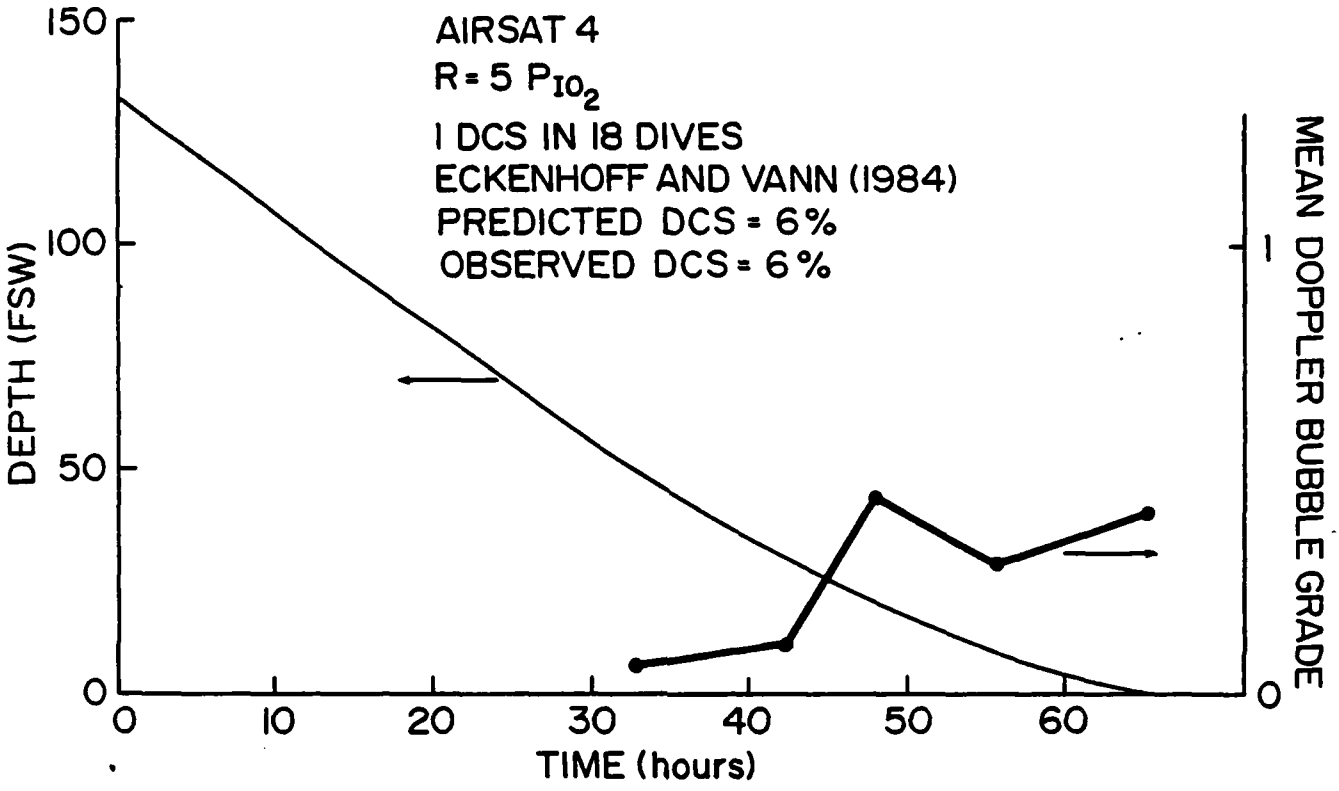
AIRSAT 4
R = 5 P_{IO_2}
1 DCS IN 18 DIVES
ECKENHOFF AND VANN (1984)
PREDICTED DCS = 6%
OBSERVED DCS = 6%
DEPTH (FSW)
150
100
50
0
0
10
20
30
40
50
60
TIME (hours)
MEAN DOPPLER BUBBLE GRADE
1
0

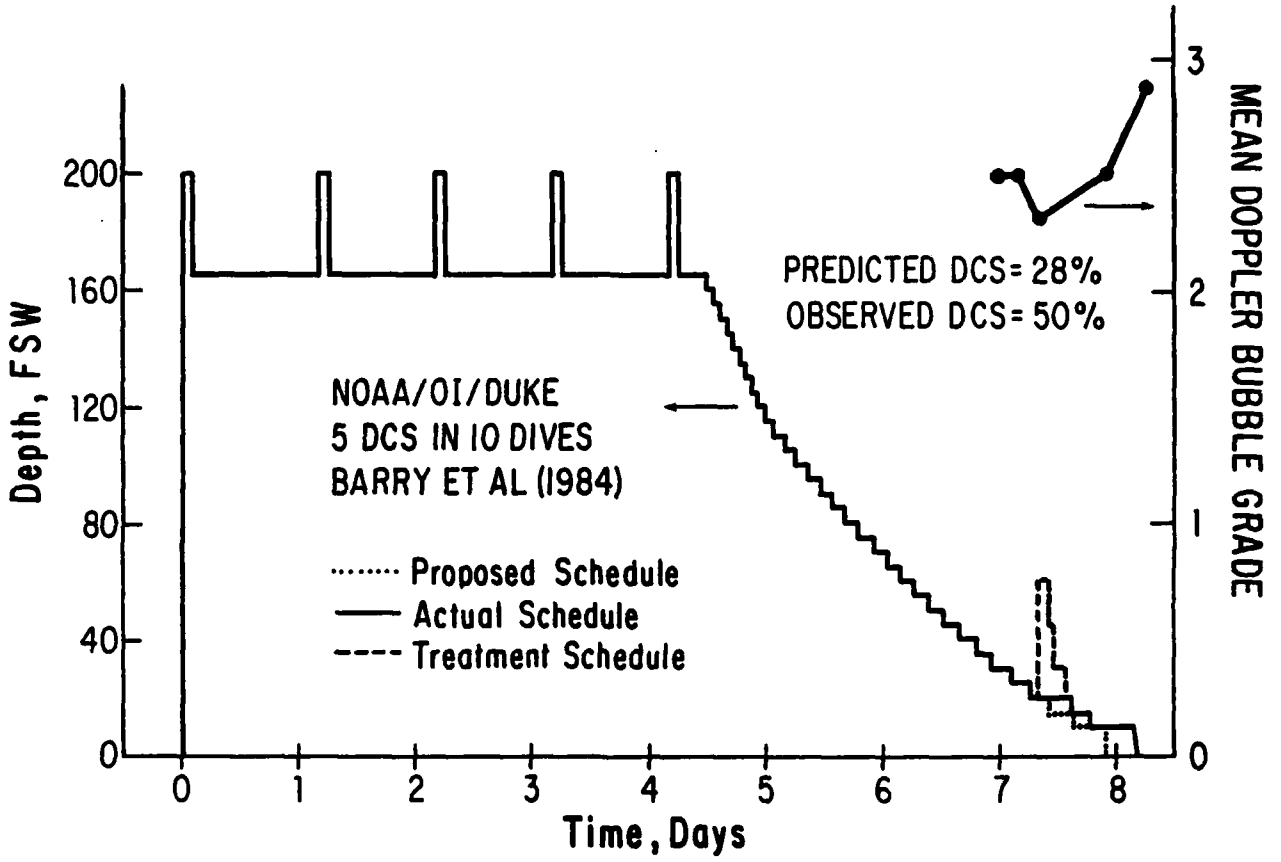
Depth, FSW
200
160
120
80
40
0
0
1
2
3
4
5
6
7
8
Time, Days
MEAN DOPPLER BUBBLE GRADE
3
2
1
0
PREDICTED DCS= 28%
OBSERVED DCS= 50%
NOAA/OI/DUKE
5 DCS IN 10 DIVES
BARRY ET AL (1984)
Proposed Schedule
Actual Schedule
Treatment Schedule

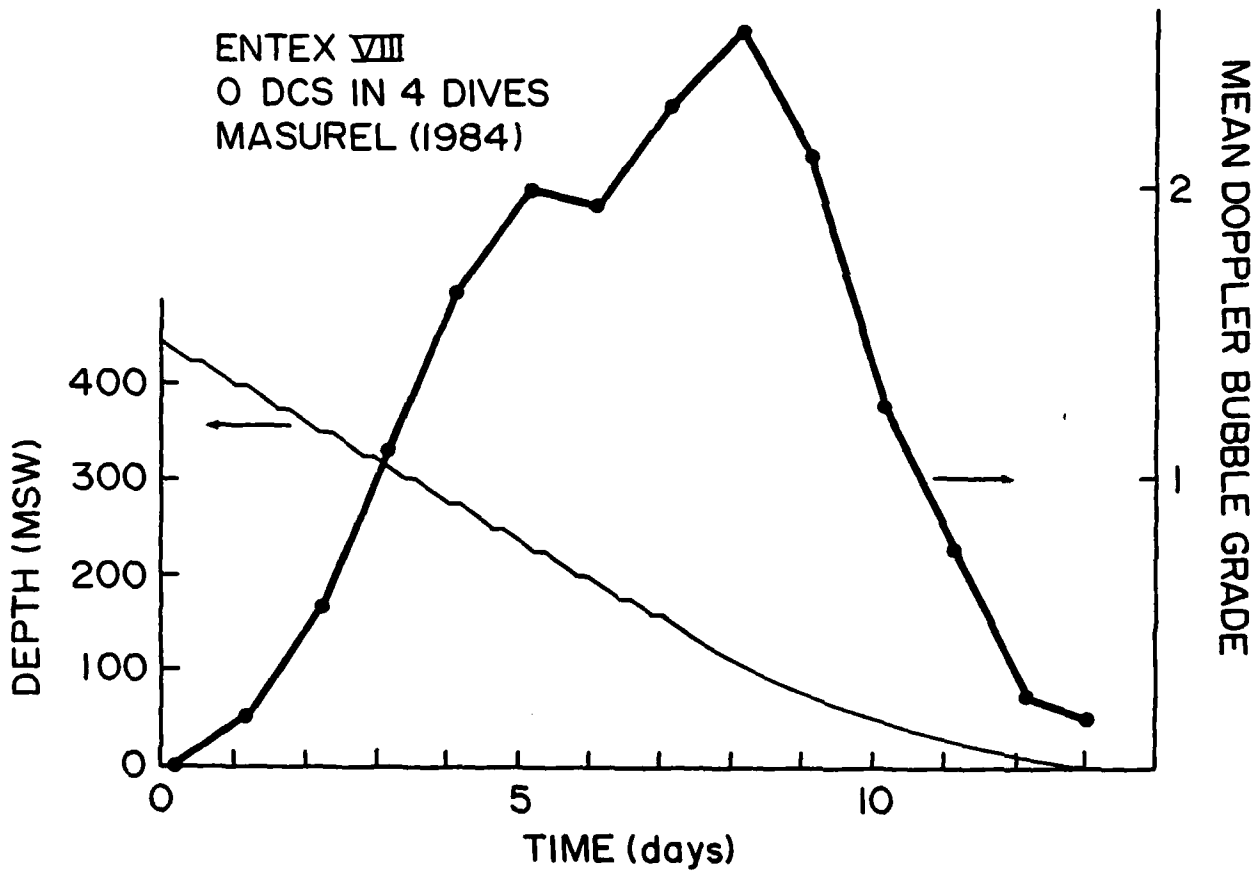
ENTEX VIII
0 DCS IN 4 DIVES
MASUREL (1984)
DEPTH (MSW)
400
300
200
100
0
0
5
10
TIME (days)
2
1
MEAN DOPPLER BUBBLE GRADE

END

FILMED

4-85

DTIC